PICL: Learning to Incorporate Physical Information When Only Coarse-Grained Data is Available

Haodong Feng[1] **Yue Wang**[2†] **Dixia Fan**[1†]
[1]School of Engineering, Westlake University,
[2]Microsoft Research,
† Corresponding authors
{fenghaodong,fandixia}@westlake.edu.cn
yuwang5@microsoft.com

Abstract

Machine learning is increasingly successful in modeling physical systems in science and engineering. Integrating physical information, like PDEs, can enhance model performance and address generalization issues caused by limited, costly data. However, since PDEs heavily rely on fine-grained states to calculate the derivative, the integration of physical information into models is significantly challenged by the coarse-grained nature of measurement, often due to sensor limitations. To address the challenge, we introduce the Physics-Informed Coarse-grained data Learning (PICL) framework to enhance the model's generalization for predicting future coarse-grained observations. The key idea is to re-enable the physics-based loss on the transition between adjacent fine-grained states corresponding to the available coarse-grained data. The challenge is how to reconstruct the corresponding fine-grained state by only using coarse-grained data. We discover that the physics-based loss can also address this challenge. PICL combines an encoding module for reconstructing learnable fine-grained states with a transition module for predicting future states. The two modules are jointly trained by data and physical information. The experiment results confirm PICL's significant improvement in generalization capacity in various physical systems.

1 Introduction

Using machine learning methods to approximate physical systems has become a promising direction in science and engineering, e.g., fluid dynamics, diffusion, and so on [41, 35]. Since the data collection procedure is always both time and cost-consuming, a limited amount of data will hurt the generalization of the physical system modeling. Recently, some works have introduced physical information (e.g., PDEs) in training models and achieved promising performance [22, 6, 9, 31, 12] to reduce the use of costly data and improve generalization capacity of physical system models. Most works rely on fine-grained data to calculate or approximate the derivative for physics-based loss, but the application of physical information for modeling physical systems is significantly challenged by the coarse-grained nature of measurement, often due to sensor limitations [13, 27, 38, 1, 14]. Computing partial derivatives in physics-based loss with coarse-grained data introduces significant biases, leading to a dilemma: either we avoid integrating physical information into the model, thereby weakening its generalization capability, or we incorporate the biased physical information, which can also hurt the model's performance. As a result, a scientific problem has been emerged:

Whether and how can we improve the model's generalization capacity by incorporating physical information when only coarse-grained data is available?

Machine Learning and the Physical Sciences Workshop, NeurIPS 2024.

In this work, we introduce a novel Physics-Informed Coarse-grained data Learning framework, known as PICL, that can effectively incorporate physical information into the training of physical system models when we only have coarse-grained data thereby enhancing the model's capacity to generalize and predict future coarse-grained observations. The core idea is that we can re-enable the physics-based loss on the transition between adjacent fine-grained states corresponding to the coarse-grained data. The challenge behind the idea is how to reconstruct the corresponding fine-grained state by only using coarse-grained observation. We find that physical information can also play a key role to solve this challenge. The PICL mainly comprises an encoding module and a transition module. The fundamental procedure is to reconstruct the learnable fine-grained state from coarse-grained observation by using the encoding module and then predict the subsequent state with the transition module. However, it is hard to train the encoding module without available fine-grained data through data-driven supervised methods. Therefore, we use several recent consecutive observations to generate a learnable fine-grained state by drawing inspiration from the PDEs formulation and finite difference method (FDM), where there exists an equivalence relation between temporal and spatial differences, allowing for interconversion between them, then train it via a physics loss.

We designed to train the encoding and transition modules jointly with two periods: a base-training period and a two-stage fine-tuning period. In base-training period, the encoding module is trained using a physics loss without requiring fine-grained data. The transition module is trained collaboratively using the data loss and physics loss to overcome the generalization issues due to data scarcity. In two-stage fine-tuning period, the framework leverages unlabeled data in a semi-supervised learning manner to further improve the model's generalization. The transition module is first fine-tuned with unlabeled data and physics loss independently; then, their information is propagated to the encoding module, which is fine-tuned using data loss calculated on the original labeled data.

Our contributions can be summarized in two parts: **(1)** We propose a general physics-informed deep learning framework called PICL to improve the model's generalization capacity by incorporating physical information if we only have coarse-grained data. **(2)** We demonstrate that PICL leads to a significant improvement in generalization for predicting the future coarse-grained observations, than baseline methods, across various physical systems.

2 Related Work

Physics-informed machine learning: More and more physics-informed machine learning methods have been proposed to learn the solutions of PDEs [16], including neural operator [26, 20–22, 36, 10, 1, 39, 14] and physics-informed neural networks (PINNs) [29, 37, 2, 16]. These works leverage physical information in constructing physics loss or network structure, thereby modeling or solving PDEs dynamics. The key to their success is the incorporation of accurate physical information, including fine-grained data or formulas of PDEs. However, they cannot be applied to learn coarse-grained data directly, as their physics-informed training manner brings significant bias when calculating coarse-grained data.

Fine-grained state reconstruction: This task aims to reconstruct a fine-grained state from its coarse-grained counterpart, also known as super-resolution in some works [43, 19]. The task mainly focuses on computer vision (CV) and physical systems. In CV, after the pioneering study by the work [3], numerous deep learning-based models [23, 33, 28, 42], and generative models [18, 25, 8] have emerged. In physical systems, the task has attracted more and more attention [31], which aims to integrate physical information into models [34, 4, 5, 15, 31, 32] or not need for data [7, 17, 40]. Among them, most rely on fine-grained data to do supervised learning; only a small part relies on physical information, thus resulting in relatively larger reconstruction errors without leveraging data information.

Different from the above related works, our framework does not require fine-grained data but rather shows that by a carefully designed framework, the physics-informed training manner can be incorporated with coarse-grained data and further improve model's generalization capacity.

3 Problem Description

We aim to use physical information to improve model's generalization for predicting future coarse-grained observations when only coarse-grained data is available in physical systems. Denote $u_t \triangleq$

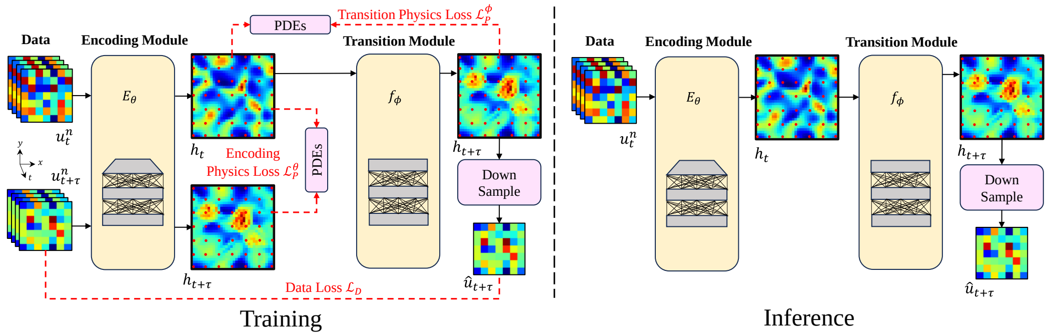

Figure 1: **PICL.** Training (left): In the base-training period, the encoding module is trained by $\mathcal{L}_D$ and $\mathcal{L}_P^{\theta}$, and the transition module is trained by $\mathcal{L}_D$ and $\mathcal{L}_P^{\phi}$. These losses are calculated on labeled dataset $\mathcal{D}$. Then, in the two-stage fine-tuning period, the transition module is tuned by $\mathcal{L}_P^{\phi}$, calculated on unlabeled dataset $\mathcal{B}$, and the encoding module is tuned by $\mathcal{L}_D$, calculated on $\mathcal{D}$, in order. Inference (right): given the coarse-grained observation to predict future coarse-grained observations.

$u(t) \in \mathcal{U}$ as a state, we want to infer $u_{t+\tau}$ for $\tau > 0$ at any time t. $\mathcal{U}$ is the functional space of form $\Omega \to \mathbb{R}^n$, where $\Omega \subset \mathbb{R}^p$ is the set of observational point location, and n is the number of system variable. That is to say, u_t is a function of $x \in \Omega$, with vectorical output $u_t(x) \in \mathbb{R}^n$. In such problems, trajectories share the same dynamics but vary by their initial conditions (ICs) $u_0 \in \mathcal{U}$. We observe a finite training set of trajectories $\mathcal{D}$ with label and $\mathcal{B}$ without label from trajectories given different ICs u_0, using a coarse-grained spatial observation grid $\mathcal{X} \subset \Omega$ on discrete times $t \in \mathcal{T} \subset [0, T]$. In inference, the coarse-grained dataset is observed with $\mathcal{X}$. Note that inference is performed on test data observed from trajectories given different ICs to verify model's generalization to different trajectories.

4 Methodology

4.1 Overview of PICL

As we mentioned in the introduction, the incorporation of physical information to model is crucial for the model generalization but is significantly challenged by coarse-grained data. To re-enable the use of physical information, PICL constructs physics loss on the transition between adjacent fine-grained states corresponding to the coarse-grained data (transition module). Furthermore, the physics loss can also help to reconstruct the corresponding fine-grained state by only using coarse-grained observation (encoding module). PICL jointly trains these two modules to effectively employ physical information to enhance the model's generalization. As shown Fig. 1 (left), there are two training periods: **Base-training period:** The encoding module is trained with a physics loss without fine-grained data, while the transition module is trained collaboratively using data loss and physics loss. **Two-stage fine-tuning period:** It utilizes unlabeled data semi-supervisedly for further improvement. The first stage involves fine-tuning (FT) transition module independently, with physics loss calculated on unlabeled data. Then, their information is propagated to encoding module in the second stage by fine-tuning with data loss calculated on original labeled data.

4.2 Model Components

We present all the model components in Fig. 1. Here we introduce each of them separately. **Encoding module:** $E_\theta(u_t^n)$. The encoding module computes the learnable fine-grained state h_t given the coarse-grained observation. We use n temporal features of $u_t^n = \{u_{t-i*\tau}\}_{i=0}^n$ to compute the more reliable h_t. **Transition module:** $f_\phi(h_t)$. After the encoding module outputs the learnable fine-grained state h_t, we then model their dynamics using a neural network. Specifically, $f_\phi : \mathbb{R}^{d_h} \to \mathbb{R}^{d_h}$ to predict the subsequent fine-grained state $h_{t+\tau}$, where d_h defines the dimensionality of the latent space. **Down-sampling:** $D(h_{t+\tau})$. Please note that data in $\mathcal{D}$ is coarse-grained, according to Fig. 1 (left), we define a down-sampling operation as $D : \mathbb{R}^{d_h} \to \mathcal{U}$ after the transition module, with the known coordinates.

Table 1: **Relative loss $\mathcal{L}_D$ (↓) and reconstruction error $\epsilon = \frac{\|\hat{h}_t - h_t\|_2}{\|h_t\|_2}$ (↓).** Our framework achieves better prediction results than all other baseline methods. Best in **bold** and second best <u>underline</u>.

Experiments		PIDL	LNPDE	GNOT	PeRCNN	FNO	FNO*	PINO*	**PICL**
Burgers	$\mathcal{L}_D$	1.43E-1	1.05E-1	1.93E-2	3.03E-1	<u>1.68E-2</u>	1.69E-2	6.35E-2	**1.37E-2**
	ϵ	<u>9.80E-6</u>	-	-	0.98	-	6.84E-5	9.81E-6	**1.85E-6**
Wave	$\mathcal{L}_D$	1.28	9.93E-1	1.33E-1	5.44E-1	1.11E-1	<u>3.58E-2</u>	1.01	**2.64E-2**
	ϵ	1.19	-	-	<u>1.18</u>	-	2.17	2.09	**1.06**
NSE	$\mathcal{L}_D$	6.45E-1	6.35E-1	1.18E-1	5.07E-1	1.06E-1	<u>1.68E-2</u>	4.70E-1	**1.34E-2**
	ϵ	1.71E-2	-	-	1.07	-	1.85E-2	<u>1.07E-2</u>	**2.76E-8**
LSWE	$\mathcal{L}_D$	7.60	9.26E-2	1.19E-1	4.92E-1	7.92E-2	<u>4.75E-2</u>	7.60	**2.44E-2**
	ϵ	**1.38E-3**	-	-	0.97	-	6.82E-3	1.63E-3	<u>1.47E-3</u>
NSWE	$\mathcal{L}_D$	2.34E-1	6.70E-2	1.63E-1	4.06E-1	1.01E-1	<u>6.41E-2</u>	2.32E-1	**3.50E-2**
	ϵ	<u>3.16E-1</u>	-	-	1.30	-	1.74	3.18E-1	**2.03E-1**

4.3 Model Learning

To overcome the challenge mentioned in the introduction when training two modules, we propose a learning strategy with two periods using the physics loss function, including a base-training period given the labeled train sequences $\mathcal{D}$ and a two-stage fine-tuning period given the unlabeled data $\mathcal{B}$.

Loss functions: We design the loss function with data loss and physics loss as follows:

$$\mathcal{L}_{PI}(\theta, \phi, \mathcal{D}) = \mathcal{L}_D(\theta, \phi, \mathcal{D}) + \gamma \mathcal{L}_P^{\theta}(\theta, \mathcal{D}) + \gamma \mathcal{L}_P^{\phi}(\phi, \mathcal{D}),$$
$$\text{where } \mathcal{L}_D(\theta, \phi, \mathcal{D}) = \frac{\|\hat{u}_{t+\tau} - u_{t+\tau}\|_2}{\|u_{t+\tau}\|_2},\ \mathcal{L}_P^{\theta}(\theta, \mathcal{D}) = F(h_t^{\theta}, h_{t+\tau}^{\theta})^2,\ \mathcal{L}_P^{\phi}(\phi, \mathcal{D}) = F(h_t^{\theta}, h_{t+\tau}^{\phi})^2, \tag{1}$$

where $\mathcal{D}$ is the labeled dataset and $(u_t, u_{t+\tau}) \in \mathcal{D}$; $\mathcal{L}_D$ is the relative l_2 data loss calculated on coarse-grained data. $\mathcal{L}_P^{\theta}$ and $\mathcal{L}_P^{\phi}$ denote the physics losses of encoding module and transition module; γ is the weight of physics loss.

Base-training period: The base-training period can be formalized as a data loss and a physics loss joint optimization problem that we solve in parallel:

$$\theta^*, \phi^* = \text{argmin}_{\theta, \phi}\ \mathcal{L}_{PI}(\theta, \phi, \mathcal{D}). \tag{2}$$

For training the encoding module to offset the complete lack of fine-grained data, we propose to encode input u_t^n and label $u_{t+\tau}^n$ to learnable fine-grained state h_t and encoded $h_{t+\tau}$ using the same encoding module, which can be used to calculate $\mathcal{L}_P^{\theta}$ in training. The derivative of $\mathcal{L}_P^{\theta}$ with respect to the parameter θ in the encoding module is calculated. To train the transition module and improve generalization for predicting, $\mathcal{L}_P^{\phi}$ is computed between the input h_t and the predicted subsequent $h_{t+\tau}$, and the derivative of $\mathcal{L}_P^{\phi}$ with respect to the parameter ϕ in the transition module is calculated.

Two-stage fine-tuning period: We leverage unlabeled data to tune both modules after the base-training period to improve model's generalization further, as shown in Fig. 1 (left). We first optimize ϕ and then optimize θ. The period can be formalized as an optimization problem:

$$\phi^* = \text{argmin}_{\phi}\ \mathcal{L}_P^{\phi}(\phi, \mathcal{B}),\ \theta^* = \text{argmin}_{\theta}\ \mathcal{L}_P^{\theta}(\theta, \mathcal{D}), \tag{3}$$

where $\mathcal{B}$ is the unlabeled dataset and the definition of $\mathcal{L}_P^{\phi}$ is same as Eqn. 1, except for $u_t \in \mathcal{B}$. Intuitively, we first fine-tune the transition module with only $\mathcal{L}_P^{\phi}$ on unlabeled data $\mathcal{B}$ to make h_t and predicted $h_{t+\tau}$ more in line with physics loss. However, as the encoding module and transition module are first trained via $\mathcal{L}_D$ together in base-training period, the fine-tuned transition module mismatches encoding module now, leading to deteriorating performance in general. Thus, we then fine-tune encoding module with $\mathcal{L}_D$ on $\mathcal{D}$. By using this order, we can propagate information of unlabeled data and physics from transition module to encoding module.

5 Experiments

We consider five PDEs which can represent common physical systems in real world: Burgers equation (Burgers), wave equation (Wave), Navier Stokes equation (NSE), linear shallow water

Table 2: Relative loss $\mathcal{L}_D$ ($\downarrow$) of the data numbers of partial observation.

$\lvert\mathcal{D}\rvert$	FNO*	**PICL**	PICL W/O FT
50	1.28E-1	**8.81E-2**	9.53E-2
100	1.07E-1	**6.88E-2**	7.34E-2
300	6.41E-2	**3.50E-2**	3.69E-2
350	5.59E-2	**3.21E-2**	3.32E-2

Table 3: Relative loss $\mathcal{L}_D$ ($\downarrow$) of the number of corresponding high-resolution states if available.

	FNO*	**PICL**
W/O HIGH-RESOLUTION STATES	6.41E-2	**3.50E-2**
WITH 1/3 HIGH-RESOLUTION STATES	5.13E-2	**3.41E-2**
WITH 1/2 HIGH-RESOLUTION STATES	5.01E-2	**3.35E-2**
WITH ALL HIGH-RESOLUTION STATES	4.70E-2	**3.29E-2**

equation (LSWE), nonlinear shallow water equation (NSWE). We compare our proposed framework with seven baselines: **PIDL**, a physics-informed deep learning approach using finite difference-based physics loss, previously applied in [24], **LNPDE** [14], **GNOT** [11], **PeRCNN** [30], **FNO** [21], **FNO*** enhancing FNO by attaching the same encoding module as in PICL, with $\gamma = 0$ in Eqn. 1, **PINO** [22], merging data and physics loss like FNO*, calculating physics loss between u_t and $u_{t+\tau}$.

As shown in Table. 1, PICL shows a significant improvement against all baselines on five benchmarks. PICL has at least 25% (against FNO* in NSE) to more than 99% (against PINO* in LSWE) improvement on $\mathcal{L}_D$ compared with all baselines. Moreover, PICL simultaneously has over 36% (against PINO* in NSWE) improvement on ϵ than most of the baselines, which means PICL can reconstruct the more accurate fine-grained state. We consider it a reason why PICL can learn the physical system models with better generalization. Note that in LSWE, reconstruction error ϵ of PIDL is slightly better than ours, but its data loss $\mathcal{L}_D$ is much larger than ours because PIDL focuses on training the model with physics loss only, ignoring the data constraint for predicting. In general, PICL achieves better performance than all baselines, which demonstrates its modeling and generalization capacity.

Furthermore, we evaluate the impact of data numbers for the partial observation $\mathcal{D}$ and high-resolution states, if available, by experiments on NSWE. **(1)** Using different numbers of trajectory $|\mathcal{D}|$, and **(2)** assuming almost 1/3, 1/2, and all partial observations have corresponding high-resolution states used as labels for the encoding module, allowing more accurate state reconstruction to explore if they can improve the performance. **(i)** Table 2 shows that $\mathcal{L}_D$ decreases as $|\mathcal{D}|$ increases; larger data volumes enhance model generalization. With less data, our framework still outperforms FNO*, although it's more effective with more data. **(ii)** Table 3 reveals that both FNO* and PICL benefit from increased high-resolution states, with PICL showing greater improvements. Please note that the relative improvement of PICL over FNO* decreases with the increase of high-resolution states, indicating PICL's function in compensating for the lack of high-resolution states.

One of the contributions of our proposed framework is that we propose the two-stage fine-tuning training strategy. It is an important part of PICL as the data scarcity tend to cause the generalization issues, especially when data acquisition is costly and only partial observation is available. We conduct the ablation study on the relationship between the data and the effect of fine-tuning. In Table 2, the PICL w/o FT means PICL is not trained by the two-stage fine-tuning period. PICL has greater improvement than PICL w/o FT when data is limited, as leveraging the unlabeled data provides additional information.

6 Conclusion

In this paper, we proposed PICL, a physics-informed coarse-grained data learning framework to re-enable the application of physical information when only coarse-grained data is available. PICL aims to improve model generalization in predicting future coarse-grained observations by using an encoding module and transition module training by the two-period strategy. Through five physical system examples, we demonstrate how incorporating physical information enhances model performance.

References

[1] Oussama Boussif, Yoshua Bengio, Loubna Benabbou, and Dan Assouline. Magnet: Mesh agnostic neural pde solver. *Advances in Neural Information Processing Systems*, 35:31972–31985, 2022.

[2] Shengze Cai, Zhiping Mao, Zhicheng Wang, Minglang Yin, and George Em Karniadakis. Physics-informed neural networks (pinns) for fluid mechanics: A review. *Acta Mechanica Sinica*, 37(12):1727–1738, 2021.

[3] Chao Dong, Chen Change Loy, Kaiming He, and Xiaoou Tang. Learning a deep convolutional network for image super-resolution. In *Computer Vision–ECCV 2014: 13th European Conference, Zurich, Switzerland, September 6-12, 2014, Proceedings, Part IV 13*, pages 184–199. Springer, 2014.

[4] Soheil Esmaeilzadeh, Kamyar Azizzadenesheli, Karthik Kashinath, Mustafa Mustafa, Hamdi A Tchelepi, Philip Marcus, Mr Prabhat, Anima Anandkumar, et al. Meshfreeflownet: A physics-constrained deep continuous space-time super-resolution framework. In *SC20: International Conference for High Performance Computing, Networking, Storage and Analysis*, pages 1–15. IEEE, 2020.

[5] Mojtaba F Fathi, Isaac Perez-Raya, Ahmadreza Baghaie, Philipp Berg, Gabor Janiga, Amirhossein Arzani, and Roshan M D'Souza. Super-resolution and denoising of 4d-flow mri using physics-informed deep neural nets. *Computer Methods and Programs in Biomedicine*, 197:105729, 2020.

[6] Han Gao, Luning Sun, and Jian-Xun Wang. Phygeonet: Physics-informed geometry-adaptive convolutional neural networks for solving parameterized steady-state pdes on irregular domain. *Journal of Computational Physics*, 428:110079, 2021.

[7] Han Gao, Luning Sun, and Jian-Xun Wang. Super-resolution and denoising of fluid flow using physics-informed convolutional neural networks without high-resolution labels. *Physics of Fluids*, 33(7), 2021.

[8] Sicheng Gao, Xuhui Liu, Bohan Zeng, Sheng Xu, Yanjing Li, Xiaoyan Luo, Jianzhuang Liu, Xiantong Zhen, and Baochang Zhang. Implicit diffusion models for continuous super-resolution. In *Proceedings of the IEEE/CVF Conference on Computer Vision and Pattern Recognition*, pages 10021–10030, 2023.

[9] Somdatta Goswami, Aniruddha Bora, Yue Yu, and George Em Karniadakis. Physics-informed deep neural operators networks. *arXiv preprint arXiv:2207.05748*, 2022.

[10] Somdatta Goswami, Minglang Yin, Yue Yu, and George Em Karniadakis. A physics-informed variational deeponet for predicting crack path in quasi-brittle materials. *Computer Methods in Applied Mechanics and Engineering*, 391:114587, 2022.

[11] Zhongkai Hao, Zhengyi Wang, Hang Su, Chengyang Ying, Yinpeng Dong, Songming Liu, Ze Cheng, Jian Song, and Jun Zhu. Gnot: A general neural operator transformer for operator learning. In *International Conference on Machine Learning*, pages 12556–12569. PMLR, 2023.

[12] Xinquan Huang, Wenlei Shi, Qi Meng, Yue Wang, Xiaotian Gao, Jia Zhang, and Tie-Yan Liu. Neuralstagger: accelerating physics-constrained neural pde solver with spatial-temporal decomposition. *arXiv preprint arXiv:2302.10255*, 2023.

[13] Valerii Iakovlev, Markus Heinonen, and Harri Lähdesmäki. Learning continuous-time pdes from sparse data with graph neural networks. *arXiv preprint arXiv:2006.08956*, 2020.

[14] Valerii Iakovlev, Markus Heinonen, and Harri Lähdesmäki. Learning space-time continuous neural pdes from partially observed states. *arXiv preprint arXiv:2307.04110*, 2023.

[15] Devendra K Jangid, Neal R Brodnik, Michael G Goebel, Amil Khan, SaiSidharth Majeti, McLean P Echlin, Samantha H Daly, Tresa M Pollock, and BS Manjunath. Adaptable physics-based super-resolution for electron backscatter diffraction maps. *npj Computational Materials*, 8(1):255, 2022.

[16] George Em Karniadakis, Ioannis G Kevrekidis, Lu Lu, Paris Perdikaris, Sifan Wang, and Liu Yang. Physics-informed machine learning. *Nature Reviews Physics*, 3(6):422–440, 2021.

[17] Daniel Kelshaw, Georgios Rigas, and Luca Magri. Physics-informed cnns for super-resolution of sparse observations on dynamical systems. *arXiv preprint arXiv:2210.17319*, 2022.

[18] Christian Ledig, Lucas Theis, Ferenc Huszár, Jose Caballero, Andrew Cunningham, Alejandro Acosta, Andrew Aitken, Alykhan Tejani, Johannes Totz, Zehan Wang, et al. Photo-realistic single image super-resolution using a generative adversarial network. In *Proceedings of the IEEE conference on computer vision and pattern recognition*, pages 4681–4690, 2017.

[19] Kehan Li, Chao Li, Baosheng Yu, Zhangchong Shen, Qiming Zhang, Shibo He, and Jiming Chen. Model and transfer spatial-temporal knowledge for fine-grained radio map reconstruction. *IEEE Transactions on Cognitive Communications and Networking*, 8(2):828–841, 2021.

[20] Zongyi Li, Nikola Kovachki, Kamyar Azizzadenesheli, Burigede Liu, Kaushik Bhattacharya, Andrew Stuart, and Anima Anandkumar. Neural operator: Graph kernel network for partial differential equations. *arXiv preprint arXiv:2003.03485*, 2020.

[21] Zongyi Li, Nikola Borislavov Kovachki, Kamyar Azizzadenesheli, Kaushik Bhattacharya, Andrew Stuart, Anima Anandkumar, et al. Fourier neural operator for parametric partial differential equations. In *International Conference on Learning Representations*, 2020.

[22] Zongyi Li, Hongkai Zheng, Nikola Kovachki, David Jin, Haoxuan Chen, Burigede Liu, Kamyar Azizzadenesheli, and Anima Anandkumar. Physics-informed neural operator for learning partial differential equations. *arXiv preprint arXiv:2111.03794*, 2021.

[23] Bee Lim, Sanghyun Son, Heewon Kim, Seungjun Nah, and Kyoung Mu Lee. Enhanced deep residual networks for single image super-resolution. In *Proceedings of the IEEE conference on computer vision and pattern recognition workshops*, pages 136–144, 2017.

[24] Xin-Yang Liu and Jian-Xun Wang. Physics-informed dyna-style model-based deep reinforcement learning for dynamic control. *Proceedings of the Royal Society A*, 477(2255):20210618, 2021.

[25] Zhi-Song Liu, Wan-Chi Siu, and Li-Wen Wang. Variational autoencoder for reference based image super-resolution. In *Proceedings of the IEEE/CVF Conference on Computer Vision and Pattern Recognition*, pages 516–525, 2021.

[26] Lu Lu, Pengzhan Jin, and George Em Karniadakis. Deeponet: Learning nonlinear operators for identifying differential equations based on the universal approximation theorem of operators. *arXiv preprint arXiv:1910.03193*, 2019.

[27] Björn Lütjens, Catherine H Crawford, Campbell D Watson, Christopher Hill, and Dava Newman. Multiscale neural operator: Learning fast and grid-independent pde solvers. *arXiv preprint arXiv:2207.11417*, 2022.

[28] Kamyar Nazeri, Harrish Thasarathan, and Mehran Ebrahimi. Edge-informed single image super-resolution. In *Proceedings of the IEEE/CVF International Conference on Computer Vision Workshops*, pages 0–0, 2019.

[29] Maziar Raissi, Paris Perdikaris, and George E Karniadakis. Physics-informed neural networks: A deep learning framework for solving forward and inverse problems involving nonlinear partial differential equations. *Journal of Computational physics*, 378:686–707, 2019.

[30] Chengping Rao, Pu Ren, Qi Wang, Oral Buyukozturk, Hao Sun, and Yang Liu. Encoding physics to learn reaction–diffusion processes. *Nature Machine Intelligence*, 5(7):765–779, 2023.

[31] Pu Ren, Chengping Rao, Yang Liu, Zihan Ma, Qi Wang, Jian-Xun Wang, and Hao Sun. Physr: Physics-informed deep super-resolution for spatiotemporal data. *Journal of Computational Physics*, 492:112438, 2023.

[32] Dule Shu, Zijie Li, and Amir Barati Farimani. A physics-informed diffusion model for high-fidelity flow field reconstruction. *Journal of Computational Physics*, 478:111972, 2023.

[33] Jae Woong Soh, Gu Yong Park, Junho Jo, and Nam Ik Cho. Natural and realistic single image super-resolution with explicit natural manifold discrimination. In *Proceedings of the IEEE/CVF conference on computer vision and pattern recognition*, pages 8122–8131, 2019.

[34] Chulin Wang, Eloisa Bentivegna, Wang Zhou, Levente Klein, and Bruce Elmegreen. Physics-informed neural network super resolution for advection-diffusion models. *arXiv preprint arXiv:2011.02519*, 2020.

[35] Hanchen Wang, Tianfan Fu, Yuanqi Du, Wenhao Gao, Kexin Huang, Ziming Liu, Payal Chandak, Shengchao Liu, Peter Van Katwyk, Andreea Deac, et al. Scientific discovery in the age of artificial intelligence. *Nature*, 620(7972):47–60, 2023.

[36] Sifan Wang, Hanwen Wang, and Paris Perdikaris. Learning the solution operator of parametric partial differential equations with physics-informed deeponets. *Science advances*, 7(40):eabi8605, 2021.

[37] Liu Yang, Xuhui Meng, and George Em Karniadakis. B-pinns: Bayesian physics-informed neural networks for forward and inverse pde problems with noisy data. *Journal of Computational Physics*, 425:109913, 2021.

[38] Yuan Yin, Matthieu Kirchmeyer, Jean-Yves Franceschi, Alain Rakotomamonjy, and Patrick Gallinari. Continuous pde dynamics forecasting with implicit neural representations. *arXiv preprint arXiv:2209.14855*, 2022.

[39] Yuan Yin, Matthieu Kirchmeyer, Jean-Yves Franceschi, Alain Rakotomamonjy, and Patrick Gallinari. Continuous pde dynamics forecasting with implicit neural representations. In *The Eleventh International Conference on Learning Representations*, 2023.

[40] Mykhaylo Zayats, Małgorzata J Zimoń, Kyongmin Yeo, and Sergiy Zhuk. Super resolution for turbulent flows in 2d: Stabilized physics informed neural networks. In *2022 IEEE 61st Conference on Decision and Control (CDC)*, pages 3377–3382. IEEE, 2022.

[41] Xuan Zhang, Limei Wang, Jacob Helwig, Youzhi Luo, Cong Fu, Yaochen Xie, Meng Liu, Yuchao Lin, Zhao Xu, Keqiang Yan, et al. Artificial intelligence for science in quantum, atomistic, and continuum systems. *arXiv preprint arXiv:2307.08423*, 2023.

[42] Hengyuan Zhao, Xiangtao Kong, Jingwen He, Yu Qiao, and Chao Dong. Efficient image super-resolution using pixel attention. In *Computer Vision–ECCV 2020 Workshops: Glasgow, UK, August 23–28, 2020, Proceedings, Part III 16*, pages 56–72. Springer, 2020.

[43] Xiangyu Zhu, Fan Yang, Di Huang, Chang Yu, Hao Wang, Jianzhu Guo, Zhen Lei, and Stan Z Li. Beyond 3dmm space: Towards fine-grained 3d face reconstruction. In *Computer Vision–ECCV 2020: 16th European Conference, Glasgow, UK, August 23–28, 2020, Proceedings, Part VIII 16*, pages 343–358. Springer, 2020.